J|A|C|S COMMUNICATIONS

Published on Web 02/04/2010

Dynamic Copper(I) Imaging in Mammalian Cells with a Genetically Encoded Fluorescent Copper(I) Sensor

Seraphine V. Wegner, Hasan Arslan, Murat Sunbul, Jun Yin, and Chuan He*

Department of Chemistry and Institute for Biophysical Dynamics, The University of Chicago, 929 East 57th Street, Chicago, Illinois, 60637, USA

Received November 16, 2009; E-mail: chuanhe@uchicago.edu

As one of the most important catalytic cofactors in proteins, copper is an essential element for life. Excess copper, however, can mis-metalate other metal binding sites; free copper catalyzes Fenton-type reactions which produce reactive oxygen species; and misregulation of copper uptake is known to cause Menkes and Wilson's disease.[1] Therefore, copper is controlled tightly by homeostatic networks in cells, which involve uptake, efflux, chaperone, and regulatory proteins.[1,2] Among the first-row transition metals, copper has an intrinsic high affinity for most ligands.[2] To prevent copper binding to other metal binding sites, the kinetically labile cellular copper is buffered to low effective concentrations due to the presence of a large number of cellular ligands, and only the high-affinity sites are able to compete for cellular copper. Therefore, in the study of copper dynamics inside the cellular setting, it is more meaningful to think of copper availability and the effective concentration of copper as buffered rather than a total concentration of copper or free copper ions.

In the cytoplasmic environment, cells sense copper availability, not the total concentration of copper, and respond accordingly. For example, the copper concentration in *Escherichia coli* has been estimated to be buffered to the order of zeptomolar based on the copper-dependent transcriptional regulator CueR which controls the expression of copper detoxification systems.[3] Likewise the copper-regulator from *Mycobacterium tuberculosis*, CsoR, shows similarly high affinity to copper(I).[4] In yeast it has been concluded that all copper ions are tightly bound inside cytoplasm on the basis of the observation that the activation of superoxide dismutase (SOD1) requires the presence of the chaperone CCS.[5] Further evidence for this hypothesis comes from tight affinities measured for copper(I) binding to copper trafficking proteins, Ccs2n, Atx1, and Ctr1c.[6]

A major challenge for copper visualization inside live cells is, as mentioned above, that cellular copper is associated with high-affinity copper binders. This makes it difficult to dynamically sample copper availability in its biological window for most copper sensors as they may not possess high enough binding constants to compete for copper within the cytoplasmic environment. A number of fluorescent small-molecule sensors for copper have been developed,[7] and a few have been used to visualize copper inside the cell.[8] However, examples thus far require incubation with high concentrations of copper which may perturb the cellular copper level beyond the biologically relevant window. Also, small-molecule sensors may have issues such as water solubility, toxicity, cell permeability, and targeting of cellular compartments. Advanced X-ray-based techniques show promising results and have been used to observe the total copper pool[9] but cannot differentiate between labile and static copper.

On the other hand, genetically encoded sensors overcome most of these limitations as they are made inside the cell. Such protein-based sensors have been very useful in the elucidation of the cellular role of calcium,[10] and more recently, new sensors to monitor zinc availability in cells have been reported;[11−13] however, a genetically encoded copper(I) sensor has been lacking. A clever design that takes advantage of the copper(I)-mediated interactions between the copper chaperone protein, Atox1, and the Wilson's disease protein's fourth domain (WD4) was reported.[12,14] Unfortunately, this sensor responds to zinc(II) as well as copper(I), and an improved version acts as an effective zinc(II) probe in mammalian cells.[13] Therefore, a system that is highly selective and sensitive to copper(I) and gives dynamic response to fluctuations in copper(I) availability in its biological window inside live cells is highly desirable.

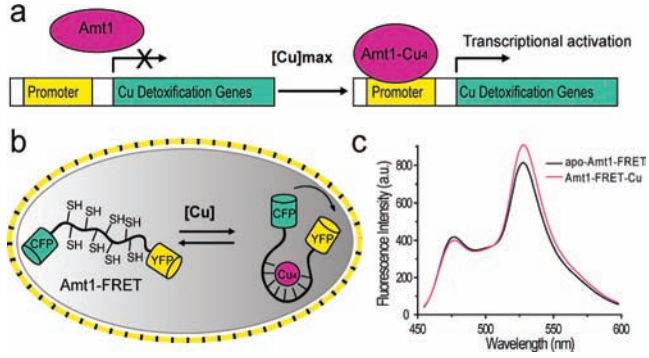

Figure 1. Design of a fluorescence reporter, Amt1-FRET for copper(I) imaging inside live cells. (a) Amt1 binds to its promoter in the presence of copper(I) to activate copper detoxification genes inside yeast cells. $[Cu]_{max}$ indicates the upper limit of copper level sensed by Amt1 in the cell. (b) The copper binding domain of Amt1 is inserted between the FRET partners CFP and YFP. At elevated copper concentration Amt1 binds copper(I) as a Cu_4 cluster. The resulting conformational change of Amt1 could induce a FRET signal change of Amt1-FRET which can be used to image copper(I) inside cells. (c) Fluorescence response of Amt1-FRET to copper(I). Apo Amt1-FRET shown in black, and Amt1-FRET with 4 equiv of copper(I) shown in purple.

Copper(I)-dependent transcriptional regulators are good starting points to design protein-based copper(I) sensors since these proteins have evolved to monitor copper availability in the cellular environment and therefore should have the right built-in affinity and selectivity. In the yeast *Candida glabrata*, the copper-dependent regulator Amt1 senses an excess of copper and activates copper detoxification/efflux genes.[15,16] Thus, the copper level as sensed by Amt1 sets the upper limit of cellular copper availability inside yeast cells (Figure 1a). Amt1 and its homologue, Ace1 in *Saccharomyces cerevisiae*, are metallothionein-like proteins which consist of three distinct domains: a zinc finger domain, a copper-binding domain, and a transactivation domain (Figure S1, Supporting Information).[17,18] The copper-binding domain (residues 36−110) contains eight cysteines involved in the formation of a tetracopper(I) cluster.[19] When the copper levels are elevated, Amt1 binds 4 equiv of copper(I), which increases its affinity for a specific promoter

DNA and activates expression of copper detoxification genes.[15,20] This reversible assembling of the copper(I) cluster induces a conformational change in Amt1 to tune its affinity to DNA.

In this study an Amt1-based copper(I) fluorescent reporter, Amt1-FRET, was constructed by subcloning the copper-binding domain of Amt1 (residues 36−110) between a cyan fluorescent protein (CFP) and a yellow fluorescent protein (YFP), taking advantage of the copper(I)-binding-induced conformational change of Amt1 (Figure 1b). This strategy, pioneered by Tsien and co-workers, produces a genetically encoded fluorescent reporter by inserting a sensing domain, which undergoes a conformational change upon target binding, between two fluorescent proteins that are fluorescence resonance energy transfer (FRET) pairs.[10,11,21]

Amt1-FRET was expressed in *E. coli* in the presence of 1.4 mM $CuSO_4$ and purified to yield the copper(I)-bound Amt1-FRET (Amt1-FRET-Cu) (Figure S2, Supporting Information). The fluorescence spectra of both copper(I)-bound and apo-Amt1-FRET were taken by exciting the FRET donor CFP (433 nm) and recording the fluorescence intensities of the YFP (527 nm) and CFP (477 nm) emissions. An increase in FRET between YFP and CFP in Amt1-FRET in the presence of Cu^+ was observed through the increase of the peak ratios (I_{527}/I_{477}) from 1.95 to 2.26 as soon as metal was added (Figure 1c), supporting the proposed copper(I)-binding-induced conformational change of Amt1 (Figure 1b). ICP-MS measurement of the purified protein sample confirmed the binding of 4 equiv of copper to Amt1-FRET (Table S1, Supporting Information). Also, reversible Cu^+ loading and removal were monitored by recording the copper(I)-thiolate charge transfer band in the UV−vis spectrum, and the measured extinction coefficient (at 280 nm) was in agreement with the literature value for the copper(I)-bound Amt1 (Figure S4, Supporting Information).[18]

Fluorescence measurements were performed to detect the binding of different metal ions to Amt1-FRET, and the result showed 4 equiv of Cu^+ binding (Figure 2a). Other than copper, Ag^+ also bound with the same stoichiometry as well as 2 equiv of Zn^{2+} and some Fe^{2+} binding to Amt1-FRET, whereas other metals that could be present inside cells, such as Ca^{2+}, Mg^{2+}, Cr^{3+}, Mn^{2+}, Co^{2+}, and Ni^{2+}, did not promote a response (Figure 2a). Furthermore, some responses from the biotoxic metal ions Cd^{2+}, Hg^{2+} and Pb^{2+} were also recorded (Figure S5, Supporting Information). Zn^{2+}, at saturation, led to only a 50% change of the maximum FRET signal change induced by Cu^+ binding to Amt1-FRET, while less than 30% FRET change was observed for the maximum binding of Fe^{2+}, Cd^{2+}, Hg^{2+}, or Pb^{2+} to Amt1-FRET. To further investigate if different metal ions interfere with the Cu^+ binding, the copper(I)-binding-induced FRET changes were measured in the presence of an equal amount of other metal ions. First, the signal for other metal ions after the addition of 5 equiv of metal to Amt1-FRET was measured, followed by the addition of an equal amount of Cu^+ (Figure 2b). In all cases, 100% of the signal was recovered, showing that Cu^+ binding is tighter compared to that of other metal ions tested and that the presence of other metal ions does not interfere with copper(I) binding to Amt1-FRET. Also, common anions were shown not to interfere with copper(I) binding (Figure S6, Supporting Information).

To establish the absolute binding selectivity and affinity of Amt1-FRET to copper(I), the FRET signal of Amt1-FRET was recorded in a series of solutions where the free Cu^+ concentration was buffered at various levels from 8.6×10^{-16} to 8.3×10^{-21} M using cyanide. For comparison, the signals of the fully copper(I)-bound form and the copper(I)-free form were also plotted at the two extremes. The binding curve, shown in Figure 2c, was obtained, and the K_d for Cu^+ binding was determined to be 2.5×10^{-18} M on the basis of the fitting of the curve. The same experiments were also conducted for Zn^{2+} binding with a series of solutions containing between 5.0×10^{-5} M to 1.3×10^{-10} M buffered Zn^{2+}. From the binding curve, the K_d for Zn^{2+} binding to Amt1-FRET was determined to be 1.4×10^{-6} M (Figure 2d). Further attempts to displace Cu^+ from Amt1-FRET by adding increasing amounts of Zn^{2+} showed no displacement even at 28 equiv Zn^{2+} (Figure S7, Supporting Information). These results demonstrate that Amt1 as well as Amt1-FRET have high selectivity toward Cu^+ and can bind copper(I) in solution where Cu^+ is buffered to attomolar concentrations, but bind only micromolar concentrations of Zn^{2+}.

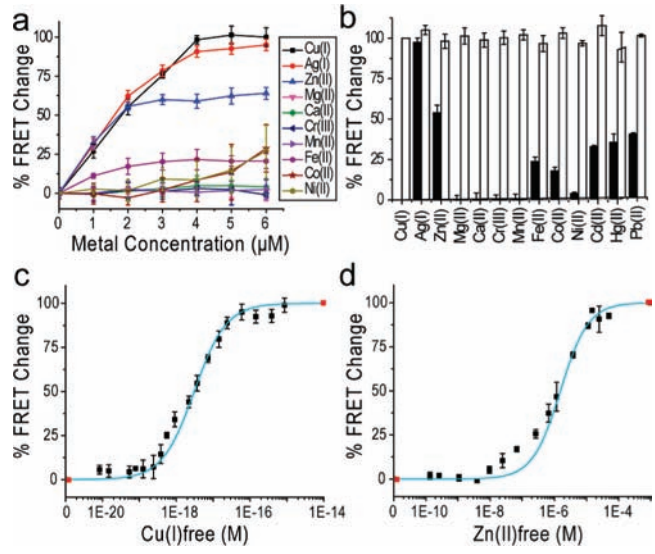

Figure 2. (a) Amt1-FRET titration with different metal ions in the presence of 4 mM DTT. Amt1-FRET (1 μM) was titrated with respective metal ion. (b) Selectivity of Amt1-FRET to Cu(I). Amt1-FRET (1 μM) with 5 μM of the respective metal ions is shown in black and the addition of 5 μM Cu(I) to the sample is shown in white. Binding curve of Amt1-FRET to (c) copper(I) and (d) zinc(II). The red points represent the maximum (Amt1-FRET-Cu or Amt1-FRET-Zn) and minimum (Apo-Amt1-FRET) FRET signals, respectively. The fitting curve is shown in blue. All measurements were done in triplicates.

To test Amt1-FRET's ability to monitor available copper inside mammalian cells CHO-K1 cells were transfected with a plasmid containing Amt1-FRET. First, the ratio of the YFP and CFP images (R_{cell}) was determined by recording the two images with excitation at the CFP absorption wavelength for an unperturbed cell (Figure 3a). Then, 100 nM $CuSO_4$ was added to the growth medium, and an image was taken after 1 min when a maximum increase of the ratio had already been observed (Figure 3b). This ratio represents the maximum ratio (R_{max}) since prolonged incubations or higher copper concentrations did not result in a further increase, suggesting that Amt1-FRET was already saturated with copper(I). Then, to find the minimum ratio (R_{min}), 2 mM of the copper(I) ligand, neocuproine,[22] was added to the cells, and the ratios of the images were taken over a 20 min period (Figure 3c−h). A decrease in the fluorescence ratio below R_{cell} was observed upon the incubation with neocuproine. These imaging results of $R_{max} > R_{cell} > R_{min}$ suggest that the unperturbed cell has a buffered copper concentration lying in the operating window of copper(I) binding to Amt1-FRET (Figure S9, Supporting Information). Further Amt1-FRET can monitor dynamic fluctuations of copper availability inside live cells since response was observed within a minute of perturbation with nanomolar levels of copper or excess chelators, avoiding prolonged incubation with micromolar concentrations of copper. This observation complements the very fast copper uptake[23] and efflux[24]

dynamics previously shown by using radioactive copper for labeling and measuring of the total copper loadings in cells.

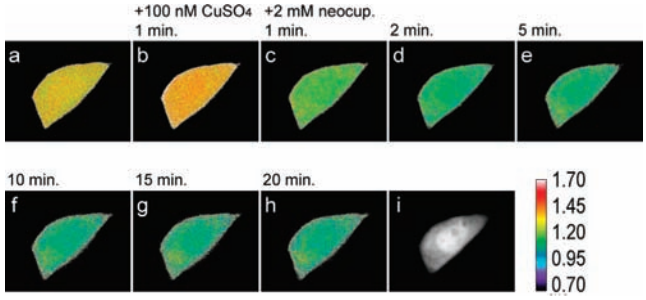

Figure 3. Imaging of available copper(I) in CHO-K1 cells by Amt1-FRET. The cells were excited at CFP, and the ratio of the YFP over CFP was taken after background corrections. (a) An unperturbed cell. (b) After one minute incubation with 100 nM $CuSO_4$. Incubation with 2 mM of neocuproine added to (b) after (c) 1 min, (d) 2 min, (e) 5 min, (f) 10 min, (g) 15 min, and (h) 20 min. (i) Fluorescence picture.

To confirm that the FRET signal observed in the unperturbed cells comes from copper(I) binding to Amt1-FRET, the response of Amt1-FRET to Zn^{2+} inside the cells was also studied. Addition of 1 μM $Zn(NO_3)_2$ to the growth medium had no effect on the FRET signal ratio measured from Amt1-FRET. In fact, an increase of FRET signaling was only observed at 10 μM or higher concentrations of Zn^{2+}. When 2 mM of a Zn^{2+} ligand EGTA was added to the cells preincubated with 10 μM Zn^{2+}, the FRET signal ratio returned to the original level but did not decrease further (Figure S4, Supporting Information). These observations indicate that the initial ratio is solely due to Cu^+ response and not to Zn^{2+}. Furthermore, when 2 mM EGTA was added to the cells preincubated with 100 nM $CuSO_4$, no change of FRET ratio was observed, thus confirming the selective Cu^+ response of Amt1-FRET inside CHO-K1 cells. A recent study showed that Zn^{2+} concentration in mammalian cells is tightly controlled at low nanomolar concentrations[13] which supports the observation that Zn^{2+} would not interfere with Cu^+ recognition by Amt1-FRET.

Our characterization of Amt1-FRET indicates that yeast copper regulators have high affinities to Cu^+ similar to those of other copper proteins from various organisms reported to date,[3−6] and copper is maintained at very low effective concentrations inside yeast. Amt1 senses elevated copper concentrations and activates the expression of metallothionein proteins in order to increase the cellular chelation capacity and to reduce available copper to healthy levels, thus setting the upper limit for cellular copper availability. In this study, a FRET-based construct (Figure 1b) was used to determine the operating window of Amt1, found to be between 2.4×10^{-19} M to 2.4×10^{-17} M for Cu^+, which places the upper limit of effective copper concentration in the yeast at about 10^{-17} M (Figure 2c). If cellular buffered copper exceeds this limit, the excess copper(I) binds to Amt1 and induces the expression of chelating proteins to reduce copper availability.

In conclusion, we constructed a FRET reporter for copper(I), taking advantage of the conformational change induced by copper(I) binding to Amt1. The resulting reporter, Amt1-FRET, is highly sensitive and selective for Cu^+ over other metal ions. The tight binding of copper(I) to Amt1-FRET supports the notion that available copper inside yeast cells is extremely limited. Copper imaging in CHO-K1 cells with the reporter suggests that the level of available copper inside mammalian cells may also be tightly controlled. This genetically encoded, ratiometric Cu^+ reporter shows great potential for imaging dynamic Cu^+ fluctuation inside mammalian cells in the biologically relevant Cu^+ concentration window. New design strategies[13] can be employed to improve the sensitivity of this sensor in the future.

Acknowledgment. We thank C. Labno and V. Bindokas at the University of Chicago, BSD Microscopy Core Facilities for their help with the imaging experiments and analyzing the data, S. Frank for editing the manuscript, Prof. D. R. Winge for the *Amt1* plasmid, and Prof. R. Y. Tsien for the AKAR1 plasmid. This work was partially supported by a CAREER award from the National Science Foundation (NSF0544546 to C.H.) and Office of Basic Energy Sciences, U.S. Department of Energy under Contract No. DE-FG02-07ER15865 (to C.H.).

Supporting Information Available: Materials and Methods, Figure S1−10, and Table S1. This material is available free of charge via the Internet at http://pubs.acs.org.

References

(1) (a) Madsen, E.; Gitlin, J. D. *Annu. Rev. Neurosci.* **2007**, *30*, 317–337. (b) Tamás, M. J.; Martinoia, E. *Molecular Biology of Metal Homeostasis and Detoxification: From Microbes to Man*. Springer: Berlin; New York, 2006; pp 1−37, 509.
(2) Waldron, K. J.; Robinson, N. J. *Nat. Rev. Microbiol.* **2009**, *7*, 25–35.
(3) Changela, A.; Chen, K.; Xue, Y.; Holschen, J.; Outten, C. E.; O'Halloran, T. V.; Mondragon, A. *Science* **2003**, *301*, 1383–1387.
(4) Liu, T.; Ramesh, A.; Ma, Z.; Ward, S. K.; Zhang, L.; George, G. N.; Talaat, A. M.; Sacchettini, J. C.; Giedroc, D. P. *Nat. Chem. Biol* **2007**, *3*, 60–68.
(5) Rae, T. D.; Schmidt, P. J.; Pufahl, R. A.; Culotta, V. C.; O'Halloran, T. V. *Science* **1999**, *284*, 805–808.
(6) Xiao, Z.; Loughlin, F.; George, G. N.; Howlett, G. J.; Wedd, A. G. *J. Am. Chem. Soc.* **2004**, *126*, 3081–3090.
(7) (a) Liu, J.; Lu, Y. *J. Am. Chem. Soc.* **2007**, *129*, 9838–9839. (b) Brunner, J.; Kraemer, R. *J. Am. Chem. Soc.* **2004**, *126*, 13626–13627. (c) Royzen, M.; Dai, Z.; Canary, J. W. *J. Am. Chem. Soc.* **2005**, *127*, 1612–1613. (d) Zhou, Z.; Fahrni, C. J. *J. Am. Chem. Soc.* **2004**, *126*, 8862–8863. (e) Romain, F. H.; Viguier, A. N. H. *J. Am. Chem. Soc.* **2006**, *128*, 11370–11371. (f) Que, E. L.; Gianolio, E.; Baker, S. L.; Wong, A. P.; Aime, S.; Chang, C. J. *J. Am. Chem. Soc.* **2009**, *131*, 8527–8536. (g) Zhao, Y.; Zhang, X. B.; Han, Z. X.; Qiao, L.; Li, C. Y.; Jian, L. X.; Shen, G. L.; Yu, R. Q. *Anal. Chem.* **2009**, *81*, 7022–7030. (h) Jung, H. S.; Kwon, P. S.; Lee, J. W.; Kim, J. I.; Hong, C. S.; Kim, J. W.; Yan, S.; Lee, J. Y.; Lee, J. H.; Joo, T.; Kim, J. S. *J. Am. Chem. Soc.* **2009**, *131*, 2008–2012.
(8) (a) Zeng, L.; Miller, E. W.; Pralle, A.; Isacoff, E. Y.; Chang, C. J. *J. Am. Chem. Soc.* **2006**, *128*, 10–11. (b) Miller, E. W.; Zeng, L.; Domaille, D. W.; Chang, C. J. *Nat. Protoc.* **2006**, *1*, 824–827.
(9) Yang, L.; McRae, R.; Henary, M. M.; Patel, R.; Lai, B.; Vogt, S.; Fahrni, C. J. *Proc. Natl. Acad. Sci. U.S.A.* **2005**, *102*, 11179–11184.
(10) (a) Miyawaki, A.; Llopis, J.; Heim, R.; McCaffery, J. M.; Adams, J. A.; Ikura, M.; Tsien, R. Y. *Nature* **1997**, *388*, 882–887. (b) Miyawaki, A.; Tsien, R. Y. *Methods Enzymol.* **2000**, *327*, 472–500.
(11) Qiao, W.; Mooney, M.; Bird, A. J.; Winge, D. R.; Eide, D. J. *Proc. Natl. Acad. Sci. U.S.A.* **2006**, *103*, 8674–8679.
(12) van Dongen, E. M.; Dekkers, L. M.; Spijker, K.; Meijer, E. W.; Klomp, L. W.; Merkx, M. *J. Am. Chem. Soc.* **2006**, *128*, 10754–10762.
(13) Vinkenborg, J. L.; Nicolson, T. J.; Bellomo, E. A.; Koay, M. S.; Rutter, G. A.; Merkx, M. *Nat. Methods* **2009**, *6*, 737–740.
(14) Wernimont, A. K.; Huffman, D. L.; Lamb, A. L.; O'Halloran, T. V.; Rosenzweig, A. C. *Nat. Struct. Biol.* **2000**, *7*, 766–771.
(15) Thorvaldsen, J. L.; Sewell, A. K.; McCowen, C. L.; Winge, D. R. *J. Biol. Chem.* **1993**, *268*, 12512–12518.
(16) Gralla, E. B.; Thiele, D. J.; Silar, P.; Valentine, J. S. *Proc. Natl. Acad. Sci. U.S.A.* **1991**, *88*, 8558–8562.
(17) Dobi, A.; Dameron, C. T.; Hu, S.; Hamer, D.; Winge, D. R. *J. Biol. Chem.* **1995**, *270*, 10171–10178.
(18) Thorvaldsen, J. L.; Sewell, A. K.; Tanner, A. M.; Peltier, J. M.; Pickering, I. J.; George, G. N.; Winge, D. R. *Biochemistry* **1994**, *33*, 9566–9577.
(19) (a) Graden, J. A.; Posewitz, M. C.; Simon, J. R.; George, G. N.; Pickering, I. J.; Winge, D. R. *Biochemistry* **1996**, *35*, 14583–14589. (b) Dameron, C. T.; Winge, D. R.; George, G. N.; Sansone, M.; Hu, S.; Hamer, D. *Proc. Natl. Acad. Sci. U.S.A.* **1991**, *88*, 6127–6131.
(20) (a) Zhou, P. B.; Thiele, D. J. *Proc. Natl. Acad. Sci. U.S.A.* **1991**, *88*, 6112–6116. (b) Furst, P.; Hu, S.; Hackett, R.; Hamer, D. *Cell* **1988**, *55*, 705–717. (c) Furst, P.; Hamer, D. *Proc. Natl. Acad. Sci. U.S.A.* **1989**, *86*, 5267–5271.
(21) Zhang, J.; Ma, Y.; Taylor, S. S.; Tsien, R. Y. *Proc. Natl. Acad. Sci. U.S.A.* **2001**, *98*, 14997–15002.
(22) (a) Byrnes, R. W.; Antholine, W. E.; Petering, D. H. *Free Rad. Biol. Med.* **1992**, *13*, 469–478. (b) Gocmen, C.; Kumcu, E. K.; Buyuknacar, H. S.; Onder, S.; Singirik, E. *Pharmacology* **2005**, *75*, 69–75.
(23) Schmitt, R. C.; Darwish, H. M.; Cheney, J. C.; Ettinger, M. J. *Am. J. Physiol.* **1983**, *244*, G183–191.
(24) Darwish, H. M.; Schmitt, R. C.; Cheney, J. C.; Ettinger, M. J. *Am. J. Physiol.* **1984**, *246*, G48–55.

JA9097324